

Research Article

Advances in Polymer Technology Application of Pareto-Based Genetic Algorithm in Determining Layout of Heating Rods for a Plastic Injection Mold

Yipeng Li, Ningning Gong , Yaohui Wang, Yuntao Chen, Bowen Wang, and Xiping Li

College of Engineering, Zhejiang Normal University, Jinhua 321004, China

Correspondence should be addressed to Ningning Gong; gnn@zjnu.cn

Received 23 June 2019; Revised 2 August 2019; Accepted 11 November 2019; Published 21 March 2020

Academic Editor: Huamin Zhou

Copyright © 2020 Yipeng Li et al. This is an open access article distributed under the Creative Commons Attribution License, which permits unrestricted use, distribution, and reproduction in any medium, provided the original work is properly cited.

The Pareto-based genetic algorithm is an effective way to solve complex optimization design problems in engineering. In this study, first, the principles of Pareto optimal solutions and multiobjective genetic algorithm were presented. Second, to investigate the influence of the mold temperature on the products' performances, a multicavity experiment injection mold was designed whose temperature could be controlled by the heating rods. To obtain a homogeneous temperature distribution across the multicavity surfaces after the heating stage, multiobjective optimization models for the heating rods layout were established based on the heat transfer process of the mold. Finally, the Pareto-based genetic algorithm and finite element method were combined to solve the optimized models to obtain the optimal solution. After a finite element analysis and experimental injection, it is proved that the optimized distribution of the heating rods in the mold is necessary for the experiment and production.

1. Introduction

Injection products quality mainly depends on the history of plastic melt experienced in the mold cavity. Mold temperature, cavity pressure, and other injection molding process parameters all play an important role in the quality of products. Especially, the mold temperature could greatly affect the melt flow process, solidification process, and the final shape and dimensional precision of the products. At suitable mold temperature, the plastic melt fills the mold cavity easily, the shrinkage and warpage of the molded part are very small, and the surface quality and mechanical properties are also relatively high. Therefore, studying and analysing the influences of the mold temperature on the product quality attaches great importance to the researchers. Lin et al. [1] investigated the effect of mold temperature field on the injection molding process of polypropylene (PP) parts. The warpage of the relevant parts due to the asymmetry of the mold temperature was examined. It was found that the part warpage decreased with the increasing mold

temperature. Zhao et al. [2, 3] analysed the effect of rapid changing mold temperature on improving microscopic feature replication and molded part appearance. The results showed that the rapid heating of the cavity helped the polymer melt to replicate the surface topography of the mold. Li et al. [4] discussed the impact of cavity surface temperature on the surface topography and texture of molded reinforced plastic parts, and it was shown that the increase of cavity surface temperature can improve the surface appearance of the injected parts. Recently, literatures [5–8] focusing on the influences of mold temperature and other parameters on the weldline properties are also attracting more attention. However, concerning the relationship between the mold temperature and the part performances, there are still many problems that are not clear. For example, the effects of the same mold temperature on different plastic materials' performances, the effects of different mold temperature on the same material performances, and especially, the formation and disappearing processes of the weldline on the injection part are still

ambiguous. Thus, it is still very necessary to do further studies on the relationship between the mold temperature and the part performances.

For this purpose, according to the American Society for Testing and Materials (ASTM) standard, an experimental injection mold with multiple cavities including tensile specimen cavity, impact specimen cavity, and bend specimen cavity was designed. Several heating rods were installed in the mold to control the mold temperature by controlling the heating time of the rods. To study different properties of the specimens in a same mold temperature, the temperature of each cavity surface must be the same and distributes uniformly before the melt injected. It is required that the installed location of the heating rods in the mold must be properly optimized. According to the characteristics of the design mold and the heat transfer process, a multiobjective model indicating the uniformity of temperature distribution and efficiency of heating mold was established by combining the finite element analysis (FEA) with Pareto's genetic algorithm (GA). Finally, the effectiveness of the proposed optimization method is proved by practical experiment.

2. Multiobjective Optimization Algorithms

2.1. Pareto Optimal Solutions. In engineering applications, conflicts often occur when it comes to optimization problems with multiobjective functions. It is foreseeable that no optimal design point can achieve optimal results for all objective functions at the same time. If an objective function is optimized with only one variable, the other parameters may be opposite to the target function value. Therefore, the traditional method of converting multiple targets into a single target by mathematical operations is greatly limited. Unlike the traditional optimization method, the weight is difficult to be clear, and the Pareto-based multiobjective optimization algorithm pays more attention to obtaining several better solutions. Designers can choose the best solution from the Pareto optimal solutions obtained according to different situations. Therefore, the Pareto optimal solution is only a compromise solution for the feasible solution domain and has been used in many engineering applications in recent years. [9–13].

2.2. Multiobjective Genetic Algorithm. The Genetic Algorithm (GA) develops on the basis of population. Every time you perform a GA operation, more than one solution can be obtained. It eliminates replacement inferior solutions by comparing them to each other in all solutions. Then, in each iteration operation, the optimal solution of the previous operation is used instead of the new variable to approximate the optimal solution. Therefore, a solution that meets certain accuracy can be considered the best solution. Therefore, GA is the same with solving multiobjective problems in engineering applications, especially the Pareto optimal solution. Poirier et al. [14] applied GA for the multiobjective optimization of steel sandwich panels under prescribed quasi-static loads. The results demonstrated that the proposed methodology could be applied to the design of light-weight

laser-welded steel sandwich panels with outstanding structural performance.

Chattaraj and Ganguli [15] used GA for multiobjective optimization. Analysis shows that for thick flexible extensions, the extended length provides a Pareto optimal solution for multiobjective optimization. Guo et al. [16] considered the differences between plants, production departments, and processes for multiobjective order scheduling in production planning in complex environments. The Pareto optimization model and the NSGA II optimization process are used to address this issue. Experiments based on industry data verify the effectiveness of the optimization model. Bandyopadhyay et al. [17] used a multiobjective genetic algorithm to simultaneously minimize the yield stress and R value to obtain the anisotropic yield function coefficients. Results showed that the yield function coefficients optimized were commendably calculating the deformation behaviour of various anisotropic metal plates. According to the literature, the GA and Pareto-based optimization are very efficient to deal with multiobjective problems. Following is an optimization process based on Pareto's multiobjective genetic algorithm. Firstly, bring design variables into the operation in the form of autosomal, which contain the information concern solutions. Secondly, the initial population composed of individuals is given default values. Next, the objective function value is used to evaluate the results of individual adaptability. By replication, crossover, and mutation, all individuals with high fitness can be passed on to the next generation to ensure genetic diversity, so as to obtain new individuals with better optimization results and finally to form a new population. Finally, the algorithm terminates when the maximum algebra is generated or the level of suitability is satisfactory. Otherwise, the process will continue to loop through the second subsequent steps until the termination condition is met. The problem presented in the current article and the details of the optimization process are described in the following text.

3. Establishment of the Optimization Model

3.1. Structure of the Experimental Injection Mold. To investigate the mold temperature influences on surface appearance, mechanical properties, and weldline formation, and disappearing process of the part, a multicavity mold including tensile, impact, and bend strength specimen is designed by the authors. Specimens with both single and double injection gates are designed for the convenience of comparing the performance of the injected part with weldline and nonweldline. Several heating rods are installed in the mold to control the mold temperature. Figure 1 shows the internal structure of the cavity.

3.2. Establishment of Multiobjective Optimization Models. For studying properties of different injection specimen with the same injection parameters, the temperature of the inner surface of the cavity should be basically the same and distributes uniformly after heating stage. For considering the

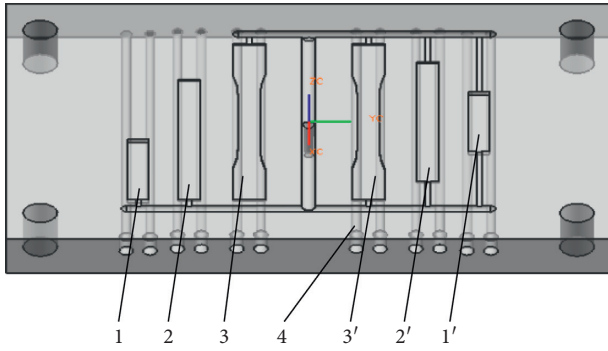


FIGURE 1: Structure of the designed mold and the standard specimen. (1, 1'): Standard tensile specimens with single gate and double gates, (2, 2'): standard bending specimens with single gate and double gates, (3, 3'): standard impact specimens with by single gate and double gates, and (4): heating rods.

experiment cost and the mold structure, two heating rods are installed under each cavity surface to heat the mold. If the interval between the two rods on the cavity does not reach an optimum distance, the temperature on the surface of the mold cavity will be inhomogeneous and the temperature difference will be large in general. Therefore, the optimization of the arrangement or position of the heaters in the cavity plate is of great significance, which can ensure the temperature distribution as well as the heating efficiency. Since the heating rods are symmetrical about the center line of the cavity plate, only half of the cavity plate cross section is set as the simplified model for studying the heat transfer process and temperature distribution analysis. The temperature distribution analysis model is shown in Figure 2.

3.2.1. Design Variables. Assuming that the interval from the heater to the surface of the cavity is the same and set to 7.5 mm, the interval from the left side to the center of each heater is set as variables to optimize the heat transfer process. Then, the lower left corner of the geometric model is set as the reference coordinate system origin. Therefore, the horizontal ordinate of the horizontal heating rod is determined as a design variable and is represented by x_i , where $i = 1-6$.

Design variables should have certain limitation before performing the optimization process. As presented in Figure 2, the boundary conditions of variables must be limited as

$$\begin{aligned} a_1 \leq x_1 \leq b_1, a_2 \leq x_2 \leq b_2, a_3 \leq x_3 \leq b_3, \\ a_4 \leq x_4 \leq b_4, a_5 \leq x_5 \leq b_5, a_6 \leq x_6 \leq b_6, \end{aligned} \quad (1)$$

where a_i, b_i ($i = 1-5$) are the lower and upper limits of the design variables, and they are defined based on the following regulations.

- (1) Based on the previous optimization results, the position of the heating rods was redefined, and the FEA model of the cavity was supplemented by the analysis of meshing and recalculation. So, the design variables should satisfy the expressions:

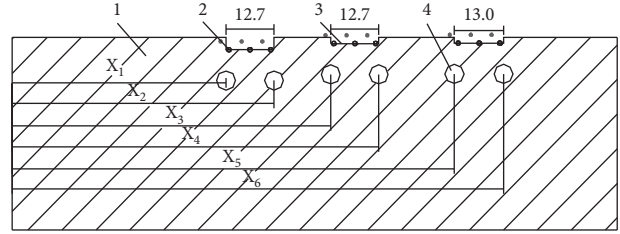


FIGURE 2: Optimization model for the designed mold (Unit: mm). 1: Cavity plate. 2: Temperature tracking points. 3: Cavity surface. 4: Heating rods.

$$b_1 + D \leq a_2, b_2 + D \leq a_3, b_3 + D \leq a_4, b_4 + D \leq a_5, b_5 + D \leq a_6, \quad (2)$$

where D represents the diameter of the heating rods. In this case, the adjacent rods will not intersect with each other in the optimization process

- (2) The two heating rods under each corresponding cavity should not be very far away from the cavity in the interest of heating efficiency

Based on the abovementioned rules and mold design experience, the boundary conditions for the design variables are defined in Table 1.

3.2.2. Objective Functions

(1) Objective Function of Heating Efficiency. To conveniently measure the temperature on the cavity surface, three suitable equidistant points are used for tracking the temperature of the cavity surface. The average value of the tracking points in determined heating time is used to define the heating efficiency. Meanwhile, the average temperature is proportional to heating time. According to the next objective function of temperature uniformity distribution, the reciprocal of average temperature can be considered as the minimum objective function. Therefore, the following function can be used to represent the objective function of heating efficiency.

$$\min F_1(X) = \min \frac{1}{\bar{T}} = \min (\text{OBJ}_w(x_1, x_2, x_3, x_4, x_5, x_6)), \quad (3)$$

where \bar{T} indicates the average value of the temperature tracking points. $X = x_1, x_2, x_3, x_4, x_5, x_6$ is a coordinate vector, and $x_1, x_2, x_3, x_4, x_5, x_6$ are design variables of vector X .

(2) Objective Function of Temperature Distribution Uniformity. In this study, the difference between the tracking point temperature and the average temperature is applied for characterizing whether the temperature distribution is uniform. The smaller the variance, the more uniform the temperature distribution. Therefore, the objective function of uniformity of temperature distribution can be expressed by the following functions:

TABLE 1: Boundary conditions of the design variables (mm).

Variables	x_1	x_2	x_3	x_4	x_5	x_6
Lower limits	60	77	92	112	132	146
Upper limits	70	85	105	125	139	155

$$\begin{aligned} \min F_2(X) &= \min \left(\sum_i^n (T_i - \bar{T})^2 \right) \\ &= \min(\text{OBJ}_f(x_1, x_2, x_3, x_4, x_5, x_6)), \end{aligned} \quad (4)$$

where, T_i is the tracking point temperature at the end of the heating stage, $i = 1, 2, \dots$ and n is used to identify the location of each temperature tracking point. $F_1(X)$ or $\text{OBJ}_w(x_1, x_2, x_3, x_4, x_5, x_6)$ and $F_2(X)$ or $\text{OBJ}_f(x_1, x_2, x_3, x_4, x_5, x_6)$ are used to represent the subobjective functions, respectively. According to the correlation characteristics of the abovementioned objective functions, it is known that, when the objective functions take a smaller value, the heating efficiency is relatively higher and the temperature distribution is much more uniform. Therefore, the parameters of the design variables should be such that the two objective functions are simultaneously minimized in order to achieve the desired value.

4. Optimization Procedure and Discussion of Results

In the present work, the optimization procedure is separated into three parts, i.e., establishing and analysing the model, simplifying the operation with clear information, and FEA simulation and Pareto-based GA optimization. Firstly, an analytical model is built by using computer-aided design software under the constraints, including initial and boundary values for design variable. Secondly, the temperature distribution on the surface of the cavity is simulated by the finite element method. For the sake of facilitating the calculation of the objective function, the corresponding subroutines are compiled and the results of temperature distribution are rearranged. Finally, the Pareto and GA-based optimization algorithms can be used to optimize the results, and the optimal values are obtained.

Considering the experiment cost and quality, P20 steel is used to manufacture the injection mold. The material properties are shown in Table 2. It is considered that these properties are invariable in the process of FEM simulation. The heating rods, which are fabricated by MISUMI cooperation, are installed in the mold, and their power is 15 w/cm².

By far, we have known all the constraints and initial variables needed before optimization beginning. Each optimization iteration is accompanied by multiple simulation operations to get better results. When optimization starts, few Pareto solutions are available to solve the problem. But, as the number of iteration increases, more and more Pareto solutions are produced. Meanwhile, much better solutions are gradually used to eliminate or replace the inferior solutions until the optimal solution of the problem is obtained.

It is easy to observe from Figure 3 that the optimal solutions of heating efficiency and uniformity of temperature distribution are obtained when the iteration operation is carried out to the 50th generation. Each point in the graph represents a Pareto optimal solution. From the figure, we can also know that the smaller the value of OBJ_w , the higher the heating efficiency, and OBJ_f is inversely related to OBJ_w . There isn't a same variable value to make both of the objective functions to be optimal at the same time. Therefore, the designer is required to select a compromise scheme to satisfy the user's requirements based on the two objective function values. Finally, FEA and experimental application verify that the optimal solution obtained in this paper meets the application requirements. The discussion is carried out in Section 5.

5. Finite Element Analysis and Experimental Application

5.1. Finite Element Analysis. From the function diagram, it is impossible to achieve optimal values for both objective functions at the same time. However, to meet the design requirement, only a compromise solution can be adopted. It was finally found that the optimized average temperature varied between 81.3°C and 90.1°C, while the OBJ_f which represents the temperature distribution uniformity varied from 67.2 to 648.2. Considering the experimental purpose, the quality of the obtained samples plays a very important role for the subsequent performance tests, and the quality of the samples mainly depends on the temperature uniformity of the mold. Besides, it is easy to improve the average temperature of the cavity surface by increasing the heating time. Therefore, it can be confirmed that the OBJ_f function plays a much more important role than the heating efficiency function. Accordingly, in the actual mold design, the variable values resulting in an optimal temperature distribution uniformity are employed. Based on the optimal design variables determined in Table 3, the optimized cavity average temperature is reduced from 84.4 (1/1.185 × 10⁻²)°C to 81.1 (1/1.233 × 10⁻²)°C. The optimized value representing temperature distribution uniformity also decreases from 561.4 to 62.8, proving that the presented optimized process is very effective. Although the uniformity of temperature distribution after optimization has been greatly improved, it inevitably leads to a slight reduction in heating efficiency, which does not affect the experimental efficiency.

Finally, FEA simulation software was used for calculating the heat transfer process of the cavity surface under different conditions. Figure 4 is a schematic diagram of simulated results by using the initial and optimized variable values, respectively. It is found that the optimized mold temperature distribution is much more uniform than the initial temperature distribution.

The temperature of the twelve tracking points before and after optimization is illustrated in Figure 5. According to the figure, the temperature of the cavity surface varies from 71.5°C to 94.7°C with the initial design variable values, and the maximum temperature difference is 23.2°C. However, after optimization, the temperature is between 78.5°C and

TABLE 2: Material properties.

Density ($\text{g}\cdot\text{cm}^{-3}$)	Specific heat, J ($\text{kg}\cdot\text{C}^{-1}$) ⁻¹	Thermal conductivity, W ($\text{m}\cdot\text{C}^{-1}$) ⁻¹	Modulus of elasticity (MPa)	Coefficient of thermal expansion ($^{\circ}\text{C}^{-1}$)
7.78	4.60×10^2	30	2.05×10^5	1.16×10^{-5}

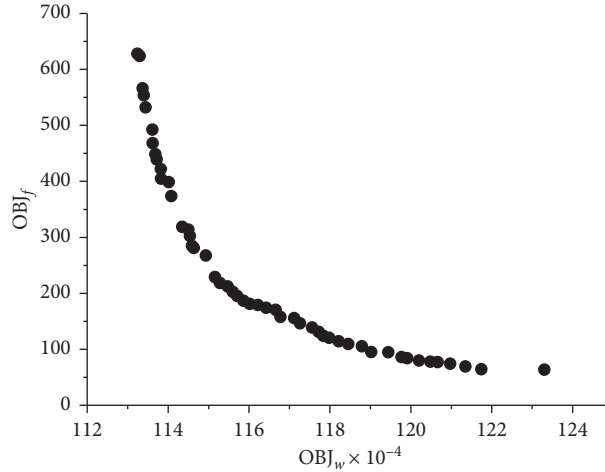


FIGURE 3: Pareto optimal solutions.

TABLE 3: Values of the initial and optimal design variables.

Design variables/objective	Initial values	Optimal values
x_1 (mm)	70.4	67.2
x_2 (mm)	84.5	78.4
x_3 (mm)	100.5	99.3
x_4 (mm)	114.5	116.2
x_5 (mm)	135.5	138.9
x_6 (mm)	149.5	153.4
Obj_f ($^{\circ}\text{C}^2$)	561.4	62.8
$(\text{Obj}_w)^{-1}$ ($^{\circ}\text{C}^{-1}$)	1.185×10^{-2}	1.233×10^{-2}

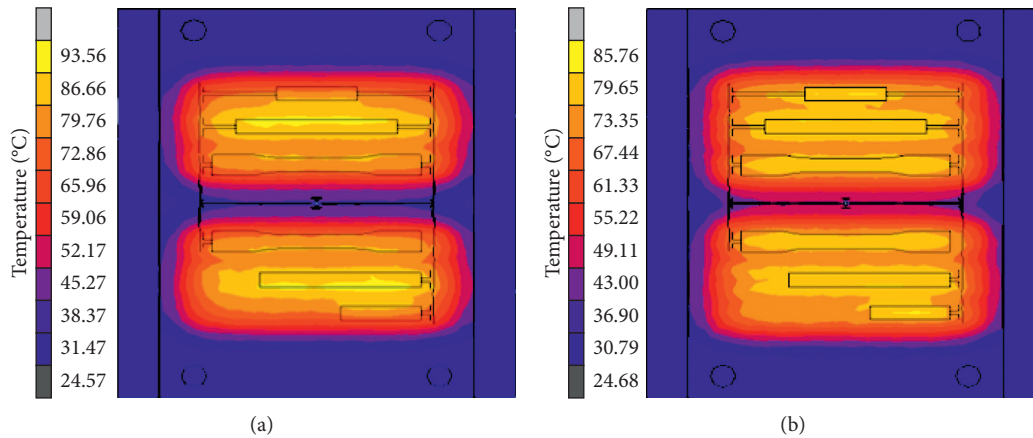


FIGURE 4: Temperature distribution of the designed mold. (a) Initial temperature distribution. (b) Optimal temperature distribution.

84.8°C, and the maximum difference in temperature is only 6.3°C. The optimized structure reduced the maximum temperature difference by 16.9°C. It can be known that the temperature value of the tracking point after optimization

is much more stable and distributed much more uniform than that of the initial mold design. Therefore, we can conclude that the optimized design is very necessary and effective.

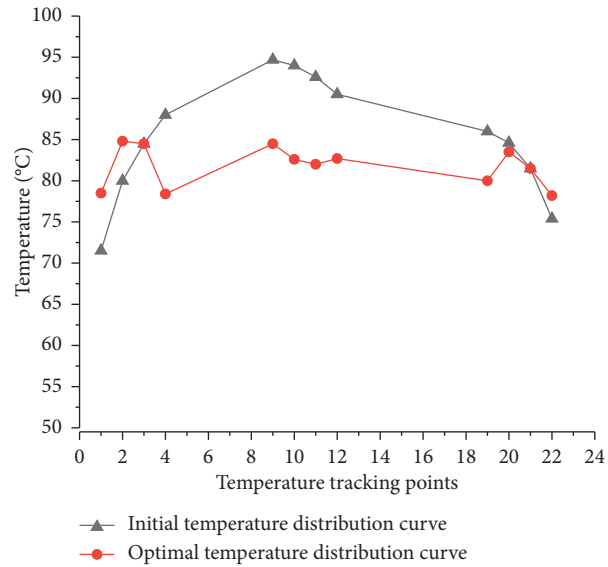


FIGURE 5: Temperature distribution curves. 1: Initial temperature distribution curve. 2: Optimal temperature distribution curve.

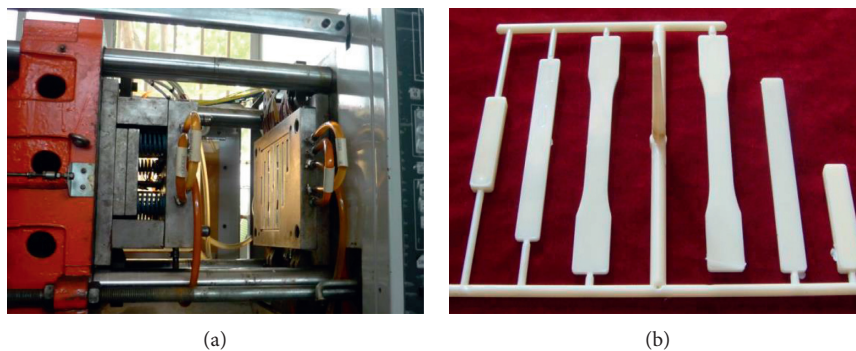


FIGURE 6: Injection experiment in the laboratory. (a) Experiment mold installed in an injection machine. (b) Produced samples.

5.2. Experiment Applications. According to the optimized results, this paper designs an experiment mold to study the influence of the mold temperature on the part performances. The layout of heating rods in the mold is designed and manufactured according to the optimized parameters. The mold temperature could be controlled by the rods, and sound samples could be successfully produced at different mold temperatures. Figure 6(a) gives the photograph of the fabricated mold in opening state installed in the injection machine in our laboratory, and Figure 6(b) shows the samples injected with a mold temperature of 85°C.

6. Conclusions

A Pareto-based multiobjective optimization method can be used to obtain a couple of optimal feasible domain compromise solutions. According to different requirements, users can choose the most efficient solution from Pareto optimal solutions. The sidedness of traditional optimization methods is avoided. By determining proper coordinates for the established model in this paper, a multiobjective model including uniform temperature distribution and the heating

efficiency of cavity surface was established. In the simulation process, an FEA method and Pareto-based GA are used to obtain optimal values of design variables. As a result, the objective function of the uniform temperature distribution reduced from 648.2 to 67.2, and the maximum temperature difference of the cavity surface is reduced from 23.2°C to 6.3°C. There is obvious improvement for the uniformity of temperature distribution. Accordingly, an experimental injection mold is designed and manufactured. Very good injection products are produced with the optimal values. The presented optimization method can also be used to solve other multiobjective problems.

Data Availability

The data used to support the findings of this study are available from the corresponding author upon request.

Conflicts of Interest

The authors declare that there are no conflicts of interest regarding the publication of this paper.

Acknowledgments

The research work was supported by the Natural Science Foundation of Zhejiang Province (LY18E050011 and LY20E050008) and National Natural Science Foundation of China (51675489).

References

- [1] Y.-H. Lin, H.-L. Chen, S.-C. Chen, and Y.-C. Lin, "Effect of asymmetric cooling system on in-mold roller injection molded part warpage," *International Communications in Heat and Mass Transfer*, vol. 61, pp. 111–117, 2015.
- [2] G. Dong, G. Zhao, L. Zhang, J. Hou, B. Li, and G. Wang, "Morphology evolution and elimination mechanism of bubble marks on surface of microcellular injection-molded parts with dynamic mold temperature control," *Industrial & Engineering Chemistry Research*, vol. 57, no. 3, pp. 1089–1101, 2017.
- [3] G. Wang, Y. Hui, L. Zhang, and G. Zhao, "Research on temperature and pressure responses in the rapid mold heating and cooling method based on annular cooling channels and electric heating," *International Journal of Heat and Mass Transfer*, vol. 116, pp. 1192–1203, 2018.
- [4] X. Li, N. Gong, Z. Gao, and C. Yang, "Fiber orientation in melt confluent process for reinforced injection molded part," *The International Journal of Advanced Manufacturing Technology*, vol. 90, no. 5-8, pp. 1457–1463, 2016.
- [5] J. Gómez-Monterde, M. Sanchez-Soto, and M. Maspoch, "Influence of injection molding parameters on the morphology mechanical and surface properties of ABS foams," *Advances in Polymer Technology*, vol. 37, no. 8, pp. 2707–2720, 2018.
- [6] K.-H. Kim, J. Cheon Park, Y. Suh, and B.-H. Koo, "Interactive robust optimal design of plastic injection products with minimum weldlines," *The International Journal of Advanced Manufacturing Technology*, vol. 88, no. 5-8, pp. 1333–1344, 2016.
- [7] C. Leisen, M. Wolf, and D. Drummer, "Influence of the mold temperature on the material properties and the vibration welding process of crosslinked polyamide 66," *Polymer Engineering & Science*, vol. 58, no. S1, pp. E207–E214, 2017.
- [8] S. Kitayama, K. Tamada, M. Takano, and S. Aiba, "Numerical optimization of process parameters in plastic injection molding for minimizing weldlines and clamping force using conformal cooling channel," *Journal of Manufacturing Processes*, vol. 32, pp. 782–790, 2018.
- [9] D. Alanis, P. Botsinis, Z. Babar et al., "A quantum-search-aided dynamic programming framework for pareto optimal routing in wireless multihop networks," *IEEE Transactions on Communications*, vol. 66, no. 8, pp. 3485–3500, 2018.
- [10] Z. Bao, X. Ren, Y. Yang, J. Zhu, C. Wang, and R. Yin, "Multi-objective integration of flexible collaborative planning and fuzzy flexible lot-splitting scheduling based on the pareto optimal," *International Journal of Hybrid Information Technology*, vol. 8, no. 7, pp. 305–318, 2015.
- [11] Y. Li, B. Feng, G. Li, J. Qi, D. Zhao, and Y. Mu, "Optimal distributed generation planning in active distribution networks considering integration of energy storage," *Applied Energy*, vol. 210, pp. 1073–1081, 2018.
- [12] J. Razmi, E. Jafarian, and S. H. Amin, "An intuitionistic fuzzy goal programming approach for finding pareto-optimal solutions to multi-objective programming problems," *Expert Systems with Applications*, vol. 65, pp. 181–193, 2016.
- [13] N. Wang, W.-J. Zhao, N. Wu, and D. Wu, "Multi-objective optimization: a method for selecting the optimal solution from Pareto non-inferior solutions," *Expert Systems with Applications*, vol. 74, pp. 96–104, 2017.
- [14] J. D. Poirier, S. S. Vel, and V. Caccese, "Multi-objective optimization of laser-welded steel sandwich panels for static loads using a genetic algorithm," *Engineering Structures*, vol. 49, pp. 508–524, 2013.
- [15] N. Chattaraj and R. Ganguli, "Multi-objective optimization of a triple layer piezoelectric bender with a flexible extension using genetic algorithm," *Mechanics of Advanced Materials and Structures*, vol. 25, no. 9, pp. 785–793, 2017.
- [16] Z. X. Guo, W. K. Wong, Z. Li, and P. Ren, "Modeling and Pareto optimization of multi-objective order scheduling problems in production planning," *Computers & Industrial Engineering*, vol. 64, no. 4, pp. 972–986, 2013.
- [17] K. Bandyopadhyay, K. Hariharan, M.-G. Lee, and Q. Zhang, "Robust multi objective optimization of anisotropic yield function coefficients," *Materials & Design*, vol. 156, pp. 184–197, 2018.